DESY 08-209

December 2008

Measurement of the charm fragmentation function in D^* photoproduction at HERA

ZEUS Collaboration

Abstract

The charm fragmentation function has been measured in D^* photoproduction with the ZEUS detector at HERA using an integrated luminosity of $120\,\mathrm{pb}^{-1}$. The fragmentation function is measured versus $z = (E + p_{\|})^{D^*}/2E^{\mathrm{jet}}$, where E is the energy of the D^* meson and $p_{\|}$ is the longitudinal momentum of the D^* meson relative to the axis of the associated jet of energy E^{jet}. Jets were reconstructed using the k_T clustering algorithm and required to have transverse energy larger than 9 GeV. The D^* meson associated with the jet was required to have a transverse momentum larger than 2 GeV. The measured function is compared to different fragmentation models incorporated in leading-logarithm Monte Carlo simulations and in a next-to-leading-order QCD calculation. The free parameters in each fragmentation model are fitted to the data. The extracted parameters and the function itself are compared to measurements from e^+e^- experiments.

The ZEUS Collaboration

S. Chekanov, M. Derrick, S. Magill, B. Musgrave, D. Nicholass[1], J. Repond, R. Yoshida
Argonne National Laboratory, Argonne, Illinois 60439-4815, USA [n]

M.C.K. Mattingly
Andrews University, Berrien Springs, Michigan 49104-0380, USA

P. Antonioli, G. Bari, L. Bellagamba, D. Boscherini, A. Bruni, G. Bruni, F. Cindolo, M. Corradi, G. Iacobucci, A. Margotti, R. Nania, A. Polini
INFN Bologna, Bologna, Italy [e]

S. Antonelli, M. Basile, M. Bindi, L. Cifarelli, A. Contin, S. De Pasquale[2], G. Sartorelli, A. Zichichi
University and INFN Bologna, Bologna, Italy [e]

D. Bartsch, I. Brock, H. Hartmann, E. Hilger, H.-P. Jakob, M. Jüngst, A.E. Nuncio-Quiroz, E. Paul, U. Samson, V. Schönberg, R. Shehzadi, M. Wlasenko
Physikalisches Institut der Universität Bonn, Bonn, Germany [b]

N.H. Brook, G.P. Heath, J.D. Morris
H.H. Wills Physics Laboratory, University of Bristol, Bristol, United Kingdom [m]

M. Kaur, P. Kaur[3], I. Singh[3]
Panjab University, Department of Physics, Chandigarh, India

M. Capua, S. Fazio, A. Mastroberardino, M. Schioppa, G. Susinno, E. Tassi
Calabria University, Physics Department and INFN, Cosenza, Italy [e]

J.Y. Kim
Chonnam National University, Kwangju, South Korea

Z.A. Ibrahim, F. Mohamad Idris, B. Kamaluddin, W.A.T. Wan Abdullah
Jabatan Fizik, Universiti Malaya, 50603 Kuala Lumpur, Malaysia [r]

Y. Ning, Z. Ren, F. Sciulli
Nevis Laboratories, Columbia University, Irvington on Hudson, New York 10027, USA [o]

J. Chwastowski, A. Eskreys, J. Figiel, A. Galas, K. Olkiewicz, B. Pawlik, P. Stopa, L. Zawiejski
The Henryk Niewodniczanski Institute of Nuclear Physics, Polish Academy of Sciences, Cracow, Poland [i]

L. Adamczyk, T. Bołd, I. Grabowska-Bołd, D. Kisielewska, J. Łukasik[4], M. Przybycień, L. Suszycki
Faculty of Physics and Applied Computer Science, AGH-University of Science and Technology, Cracow, Poland [p]

A. Kotański[5], W. Słomiński[6]
Department of Physics, Jagellonian University, Cracow, Poland

O. Behnke, U. Behrens, C. Blohm, A. Bonato, K. Borras, D. Bot, R. Ciesielski, N. Coppola, S. Fang, J. Fourletova[7], A. Geiser, P. Göttlicher[8], J. Grebenyuk, I. Gregor, T. Haas, W. Hain, A. Hüttmann, F. Januschek, B. Kahle, I.I. Katkov[9], U. Klein[10], U. Kötz, H. Kowalski, M. Lisovyi, E. Lobodzinska, B. Löhr, R. Mankel[11], I.-A. Melzer-Pellmann, S. Miglioranzi[12], A. Montanari, T. Namsoo, D. Notz[11], A. Parenti, L. Rinaldi[13], P. Roloff, I. Rubinsky, U. Schneekloth, A. Spiridonov[14], D. Szuba[15], J. Szuba[16], T. Theedt, J. Ukleja[17], G. Wolf, K. Wrona, A.G. Yagües Molina, C. Youngman, W. Zeuner[11]
Deutsches Elektronen-Synchrotron DESY, Hamburg, Germany

V. Drugakov, W. Lohmann, S. Schlenstedt
Deutsches Elektronen-Synchrotron DESY, Zeuthen, Germany

G. Barbagli, E. Gallo
INFN Florence, Florence, Italy [e]

P. G. Pelfer
University and INFN Florence, Florence, Italy [e]

A. Bamberger, D. Dobur, F. Karstens, N.N. Vlasov[18]
Fakultät für Physik der Universität Freiburg i.Br., Freiburg i.Br., Germany [b]

P.J. Bussey[19], A.T. Doyle, W. Dunne, M. Forrest, M. Rosin, D.H. Saxon, I.O. Skillicorn
Department of Physics and Astronomy, University of Glasgow, Glasgow, United Kingdom [m]

I. Gialas[20], K. Papageorgiu
Department of Engineering in Management and Finance, Univ. of Aegean, Greece

U. Holm, R. Klanner, E. Lohrmann, H. Perrey, P. Schleper, T. Schörner-Sadenius, J. Sztuk, H. Stadie, M. Turcato
Hamburg University, Institute of Exp. Physics, Hamburg, Germany [b]

C. Foudas, C. Fry, K.R. Long, A.D. Tapper
Imperial College London, High Energy Nuclear Physics Group, London, United Kingdom [m]

T. Matsumoto, K. Nagano, K. Tokushuku[21], S. Yamada, Y. Yamazaki[22]
Institute of Particle and Nuclear Studies, KEK, Tsukuba, Japan [f]

A.N. Barakbaev, E.G. Boos, N.S. Pokrovskiy, B.O. Zhautykov
Institute of Physics and Technology of Ministry of Education and Science of Kazakhstan, Almaty, Kazakhstan

V. Aushev[23], O. Bachynska, M. Borodin, I. Kadenko, A. Kozulia, V. Libov, D. Lontkovskyi, I. Makarenko, Iu. Sorokin, A. Verbytskyi, O. Volynets
Institute for Nuclear Research, National Academy of Sciences, Kiev and Kiev National University, Kiev, Ukraine

D. Son
Kyungpook National University, Center for High Energy Physics, Daegu, South Korea [g]

J. de Favereau, K. Piotrzkowski
Institut de Physique Nucléaire, Université Catholique de Louvain, Louvain-la-Neuve, Belgium [q]

F. Barreiro, C. Glasman, M. Jimenez, L. Labarga, J. del Peso, E. Ron, M. Soares, J. Terrón, C. Uribe-Estrada *Departamento de Física Teórica, Universidad Autónoma de Madrid, Madrid, Spain* [l]

F. Corriveau, C. Liu, J. Schwartz, R. Walsh, C. Zhou
Department of Physics, McGill University, Montréal, Québec, Canada H3A 2T8 [a]

T. Tsurugai
Meiji Gakuin University, Faculty of General Education, Yokohama, Japan [f]

A. Antonov, B.A. Dolgoshein, D. Gladkov, V. Sosnovtsev, A. Stifutkin, S. Suchkov
Moscow Engineering Physics Institute, Moscow, Russia [j]

R.K. Dementiev, P.F. Ermolov †, L.K. Gladilin, Yu.A. Golubkov, L.A. Khein, I.A. Korzhavina, V.A. Kuzmin, B.B. Levchenko[24], O.Yu. Lukina, A.S. Proskuryakov, L.M. Shcheglova, D.S. Zotkin
Moscow State University, Institute of Nuclear Physics, Moscow, Russia [k]

I. Abt, A. Caldwell, D. Kollar, B. Reisert, W.B. Schmidke
Max-Planck-Institut für Physik, München, Germany

G. Grigorescu, A. Keramidas, E. Koffeman, P. Kooijman, A. Pellegrino, H. Tiecke, M. Vázquez[12], L. Wiggers
NIKHEF and University of Amsterdam, Amsterdam, Netherlands [h]

N. Brümmer, B. Bylsma, L.S. Durkin, A. Lee, T.Y. Ling
Physics Department, Ohio State University, Columbus, Ohio 43210, USA [n]

P.D. Allfrey, M.A. Bell, A.M. Cooper-Sarkar, R.C.E. Devenish, J. Ferrando, B. Foster, C. Gwenlan[25], K. Horton[26], K. Oliver, A. Robertson, R. Walczak
Department of Physics, University of Oxford, Oxford United Kingdom [m]

A. Bertolin, F. Dal Corso, S. Dusini, A. Longhin, L. Stanco
INFN Padova, Padova, Italy [e]

P. Bellan, R. Brugnera, R. Carlin, A. Garfagnini, S. Limentani
Dipartimento di Fisica dell' Università and INFN, Padova, Italy [e]

B.Y. Oh, A. Raval, J.J. Whitmore[27]
Department of Physics, Pennsylvania State University, University Park, Pennsylvania 16802 [o]

Y. Iga
Polytechnic University, Sagamihara, Japan [f]

G. D'Agostini, G. Marini, A. Nigro
Dipartimento di Fisica, Università 'La Sapienza' and INFN, Rome, Italy [e]

J.E. Cole[28], J.C. Hart
Rutherford Appleton Laboratory, Chilton, Didcot, Oxon, United Kingdom [m]

H. Abramowicz[29], R. Ingbir, S. Kananov, A. Levy, A. Stern
Raymond and Beverly Sackler Faculty of Exact Sciences, School of Physics, Tel Aviv University, Tel Aviv, Israel [d]

M. Kuze, J. Maeda
Department of Physics, Tokyo Institute of Technology, Tokyo, Japan [f]

R. Hori, S. Kagawa[30], N. Okazaki, S. Shimizu, T. Tawara
Department of Physics, University of Tokyo, Tokyo, Japan [f]

R. Hamatsu, H. Kaji[31], S. Kitamura[32], O. Ota[33], Y.D. Ri
Tokyo Metropolitan University, Department of Physics, Tokyo, Japan [f]

M. Costa, M.I. Ferrero, V. Monaco, R. Sacchi, V. Sola, A. Solano
Università di Torino and INFN, Torino, Italy [e]

M. Arneodo, M. Ruspa
Università del Piemonte Orientale, Novara, and INFN, Torino, Italy [e]

S. Fourletov[7], J.F. Martin, T.P. Stewart
Department of Physics, University of Toronto, Toronto, Ontario, Canada M5S 1A7 [a]

S.K. Boutle[20], J.M. Butterworth, T.W. Jones, J.H. Loizides, M. Wing[34]
Physics and Astronomy Department, University College London, London, United Kingdom [m]

B. Brzozowska, J. Ciborowski[35], G. Grzelak, P. Kulinski, P. Łużniak[36], J. Malka[36], R.J. Nowak, J.M. Pawlak, W. Perlanski[36], T. Tymieniecka[37], A.F. Żarnecki
Warsaw University, Institute of Experimental Physics, Warsaw, Poland

M. Adamus, P. Plucinski[38], A. Ukleja
Institute for Nuclear Studies, Warsaw, Poland

Y. Eisenberg, D. Hochman, U. Karshon
Department of Particle Physics, Weizmann Institute, Rehovot, Israel [c]

E. Brownson, D.D. Reeder, A.A. Savin, W.H. Smith, H. Wolfe
Department of Physics, University of Wisconsin, Madison, Wisconsin 53706, USA [n]

S. Bhadra, C.D. Catterall, Y. Cui, G. Hartner, S. Menary, U. Noor, J. Standage, J. Whyte
Department of Physics, York University, Ontario, Canada M3J 1P3 [a]

[1] also affiliated with University College London, United Kingdom
[2] now at University of Salerno, Italy
[3] also working at Max Planck Institute, Munich, Germany
[4] now at Institute of Aviation, Warsaw, Poland
[5] supported by the research grant no. 1 P03B 04529 (2005-2008)
[6] This work was supported in part by the Marie Curie Actions Transfer of Knowledge project COCOS (contract MTKD-CT-2004-517186)
[7] now at University of Bonn, Germany
[8] now at DESY group FEB, Hamburg, Germany
[9] also at Moscow State University, Russia
[10] now at University of Liverpool, UK
[11] on leave of absence at CERN, Geneva, Switzerland
[12] now at CERN, Geneva, Switzerland
[13] now at Bologna University, Bologna, Italy
[14] also at Institut of Theoretical and Experimental Physics, Moscow, Russia
[15] also at INP, Cracow, Poland
[16] also at FPACS, AGH-UST, Cracow, Poland
[17] partially supported by Warsaw University, Poland
[18] partly supported by Moscow State University, Russia
[19] Royal Society of Edinburgh, Scottish Executive Support Research Fellow
[20] also affiliated with DESY, Germany
[21] also at University of Tokyo, Japan
[22] now at Kobe University, Japan
[23] supported by DESY, Germany
[24] partly supported by Russian Foundation for Basic Research grant no. 05-02-39028-NSFC-a
[25] STFC Advanced Fellow
[26] nee Korcsak-Gorzo
[27] This material was based on work supported by the National Science Foundation, while working at the Foundation.
[28] now at University of Kansas, Lawrence, USA
[29] also at Max Planck Institute, Munich, Germany, Alexander von Humboldt Research Award
[30] now at KEK, Tsukuba, Japan
[31] now at Nagoya University, Japan
[32] member of Department of Radiological Science, Tokyo Metropolitan University, Japan
[33] now at SunMelx Co. Ltd., Tokyo, Japan
[34] also at Hamburg University, Inst. of Exp. Physics, Alexander von Humboldt Research Award and partially supported by DESY, Hamburg, Germany

[35] also at Łódź University, Poland
[36] member of Łódź University, Poland
[37] also at University of Podlasie, Siedlce, Poland
[38] now at Lund Universtiy, Lund, Sweden
† deceased

[a] supported by the Natural Sciences and Engineering Research Council of Canada (NSERC)

[b] supported by the German Federal Ministry for Education and Research (BMBF), under contract numbers 05 HZ6PDA, 05 HZ6GUA, 05 HZ6VFA and 05 HZ4KHA

[c] supported in part by the MINERVA Gesellschaft für Forschung GmbH, the Israel Science Foundation (grant no. 293/02-11.2) and the U.S.-Israel Binational Science Foundation

[d] supported by the Israel Science Foundation

[e] supported by the Italian National Institute for Nuclear Physics (INFN)

[f] supported by the Japanese Ministry of Education, Culture, Sports, Science and Technology (MEXT) and its grants for Scientific Research

[g] supported by the Korean Ministry of Education and Korea Science and Engineering Foundation

[h] supported by the Netherlands Foundation for Research on Matter (FOM)

[i] supported by the Polish State Committee for Scientific Research, project no. DESY/256/2006 - 154/DES/2006/03

[j] partially supported by the German Federal Ministry for Education and Research (BMBF)

[k] supported by RF Presidential grant N 1456.2008.2 for the leading scientific schools and by the Russian Ministry of Education and Science through its grant for Scientific Research on High Energy Physics

[l] supported by the Spanish Ministry of Education and Science through funds provided by CICYT

[m] supported by the Science and Technology Facilities Council, UK

[n] supported by the US Department of Energy

[o] supported by the US National Science Foundation. Any opinion, findings and conclusions or recommendations expressed in this material are those of the authors and do not necessarily reflect the views of the National Science Foundation.

[p] supported by the Polish Ministry of Science and Higher Education as a scientific project (2006-2008)

[q] supported by FNRS and its associated funds (IISN and FRIA) and by an Inter-University Attraction Poles Programme subsidised by the Belgian Federal Science Policy Office

[r] supported by an FRGS grant from the Malaysian government

1 Introduction

The production of a charm hadron is described as the convolution of the perturbative production of a charm quark and the non-perturbative transition of a charm quark to a hadron. The non-perturbative component is assumed to be universal, i.e. independent of the initial conditions. It is described by so-called fragmentation functions which parametrise the transfer of the quark's energy to a given hadron. The free parameters are determined from fits to data. The transition of a charm quark to a D^* meson is the subject of this paper.

The parameters of the various fragmentation function ansätze were so far derived from data obtained at e^+e^- colliders. The e^+e^- data span a wide range of centre-of-mass energies and the fragmentation of a charm quark to a D^* meson has been measured many times [1], most recently by the CLEO [2] and Belle [3] collaborations at a centre-of-mass energy of $\sim$10.5 GeV and the ALEPH [4] collaboration at 91.2 GeV. Due to scaling violations in QCD, the dependence of the fragmentation function on production energy [1, 5] is expected to follow the DGLAP equations [6].

The fragmentation function has recently been measured by the H1 Collaboration for the production of D^* mesons in deep inelastic scattering (DIS) [7]. A measurement of the fragmentation function at HERA and its comparison with that deduced from experiments at e^+e^- colliders provides a measure of the universality of charm fragmentation and further constrains its form. The analysis presented here has been performed in the photoproduction regime in which a quasi-real photon of low virtuality, Q^2, is emitted from the incoming electron or positron and collides with a parton in the proton.

2 Experimental conditions

The analysis was performed using data collected with the ZEUS detector at HERA during 1996–2000. In this period, HERA collided electrons or positrons with energy $E_e = 27.5\,\text{GeV}$ and protons with energy $E_p = 820\,\text{GeV}$ (1996–1997) or $E_p = 920\,\text{GeV}$ (1998–2000) corresponding to integrated luminosities of 38.6 ± 0.6 and $81.9 \pm 1.8\,\text{pb}^{-1}$ and to centre-of-mass energies $\sqrt{s} = 300\,\text{GeV}$ and $\sqrt{s} = 318\,\text{GeV}$, respectively.

A detailed description of the ZEUS detector can be found elsewhere [8]. A brief outline of the components that are most relevant for this analysis is given below.

Charged particles were tracked in the central tracking detector (CTD) [9], which operated in a magnetic field of 1.43 T provided by a thin superconducting coil. The CTD consisted

of 72 cylindrical drift chamber layers, organised in 9 superlayers covering the polar-angle[1] region $15^\circ < \theta < 164^\circ$. The transverse-momentum resolution for full-length tracks was $\sigma(p_T)/p_T = 0.0058 p_T \oplus 0.0065 \oplus 0.0014/p_T$, with p_T in GeV.

The high-resolution uranium–scintillator calorimeter (CAL) [10] consisted of three parts: the forward (FCAL), the barrel (BCAL) and the rear (RCAL) calorimeters. Each part was subdivided transversely into towers and longitudinally into one electromagnetic section (EMC) and either one (in RCAL) or two (in BCAL and FCAL) hadronic sections (HAC). The smallest subdivision of the calorimeter was called a cell. The CAL energy resolutions, as measured under test-beam conditions, were $\sigma(E)/E = 0.18/\sqrt{E}$ for electrons and $\sigma(E)/E = 0.35/\sqrt{E}$ for hadrons, with E in GeV.

The luminosity was measured from the rate of the bremsstrahlung process $ep \rightarrow e\gamma p$, where the photon was measured in a lead–scintillator calorimeter [11] placed in the HERA tunnel at $Z = -107$ m.

3 Event selection and reconstruction

A three-level trigger system was used to select events online [8, 12, 13]. At the first- and second-level triggers, general characteristics of photoproduction events were required and background due to beam-gas interactions rejected. At the third level, a version of the tracking information close to the offline version was used to select D^* candidates.

Kinematic variables and jets were reconstructed offline using a combination of track and calorimeter information that optimises the resolution of reconstructed kinematic variables [14]. A selected track or calorimeter cluster is referred to as an Energy Flow Object (EFO). The jets were reconstructed with the k_T cluster algorithm [15] in its longitudinally invariant inclusive mode [16], where the parameter R is chosen equal to 1. Jets were formed from the EFOs with at least one jet required to have transverse energy, $E_T^{\rm jet} > 9\,\text{GeV}$ and pseudorapidity, $|\eta^{\rm jet}| < 2.4$. The photon-proton centre-of-mass energy, $W_{\gamma p}$, was calculated using the formula $W_{\gamma p} = \sqrt{2E_p(\sum_i E_i - p_{Z,i})}$, where the sum runs over the energy and longitudinal momentum component of all EFOs. Due to trigger requirements and beam-gas background at low $W_{\gamma p}$ and background from DIS events at high $W_{\gamma p}$, the requirement $130 < W_{\gamma p} < 280\,\text{GeV}$ was made. Neutral current DIS events

[1] The ZEUS coordinate system is a right-handed Cartesian system, with the Z axis pointing in the proton beam direction, referred to as the "forward direction", and the X axis pointing left towards the centre of HERA. The coordinate origin is at the nominal interaction point. The pseudorapidity is defined as $\eta = -\ln\left(\tan\frac{\theta}{2}\right)$, where the polar angle, θ, is measured with respect to the proton beam direction.

with a scattered electron or positron candidate in the CAL were also removed by cutting [17] on the inelasticity, y, which is estimated from the energy, E'_e, and polar angle, θ'_e, of the scattered electron or positron candidate using $y_e = 1 - \frac{E'_e}{2E_e}(1 - \cos\theta'_e)$. Events were rejected if $y_e < 0.7$.

The D^* mesons were identified using the decay channel $D^{*+} \to D^0\pi_s^+$ with the subsequent decay $D^0 \to K^-\pi^+$ and the corresponding anti-particle decay. They were reconstructed from charged tracks in the CTD using the mass-difference technique [18]. Tracks with opposite charges and transverse momenta greater than 0.5 GeV were combined into pairs to form D^0 candidates. No particle identification was used, so kaon and pion masses were assumed in turn for each track to calculate the invariant mass $M(K\pi)$. A third track, assumed to be the soft pion, π_s^+, with transverse momentum greater than 0.12 GeV and of opposite charge to the kaon, was combined to form a D^* candidate with invariant mass $M(K\pi\pi_s)$. The D^* candidates were then required to have $p_T^{D^*} > 2$ GeV and $|\eta^{D^*}| < 1.5$.

To minimise background, narrow windows were selected for the mass difference, $\Delta M = M(K\pi\pi_s) - M(K\pi)$, and the mass of the D^0 meson: $0.1435 < \Delta M < 0.1475$ GeV and $1.83 < M(D^0) < 1.90$ GeV. For background determination, D^0 candidates with wrong-charge combinations, in which both tracks forming the D^0 candidates have the same charge and the third track has the opposite charge, were also retained. The same kinematic restrictions were applied as for those D^0 candidates with correct-charge combinations. The normalisation factor of the wrong-charge sample (a value of 1.02 for the distribution after all requirements shown in Fig. 1) was determined as the ratio of events with correct-charge combinations to wrong-charge combinations in the region $0.150 < \Delta M < 0.165$ GeV. A cut of $p_T^{D^*}/E_\perp^{\theta>10^\circ} > 0.1$ was imposed to further reduce combinatorial background, where $E_\perp^{\theta>10^\circ}$ is the transverse energy measured using all EFOs outside a cone of 10° in the forward direction. The forward region was excluded because of the strong influence of the proton remnant [19].

Finally, the D^* meson was associated with the closest jet (with $E_T^{\rm jet} > 9$ GeV and $|\eta^{\rm jet}| < 2.4$) in $\eta - \phi$ space and requiring $R\left(= \sqrt{(\eta^{\rm jet} - \eta^{D^*})^2 + (\phi^{\rm jet} - \phi^{D^*})^2}\right) < 0.6$.

The combined efficiency for all the above requirements was about 35%. A clear D^* mass peak above a relatively small background is shown in Fig. 1. Subtraction of the background of 634 ± 30 candidates, estimated from the wrong-charge sample, gave 1307 ± 53 D^* mesons. The background was subtracted bin-by-bin as a function of the measured fragmentation variable and all other subsequent distributions.

4 Fragmentation variables and kinematic region

In e^+e^- collisions, at leading order (LO), the two produced charm quarks each carry half of the available centre-of-mass energy, $\sqrt{s}$. The fragmentation variable of a D^* meson can therefore be simply related to one of the two produced jets. In ep collisions, the definition of the fragmentation variable is not so simple as only a fraction of the available centre-of-mass energy contributes to the production of charm quarks in the hard scattering process. However, charm quarks produced in the hard scatter form final-state jets of which the meson is a constituent. Therefore, the fragmentation variable, z, is calculated as $z = (E + p_\parallel)^{D^*}/(E + p_\parallel)^{\rm jet}$, where $p_\parallel$ is the longitudinal momentum of the D^* meson or of the jet relative to the axis of the associated jet of energy, $E^{\rm jet}$, where all quantities are given in the laboratory frame. As the jets are reconstructed as massless objects, z simplifies to:

$$z = (E + p_\parallel)^{D^*}/2E^{\rm jet}. \tag{1}$$

The analysis was performed in the photoproduction regime with $130 < W_{\gamma p} < 280\,\text{GeV}$ and $Q^2 < 1\,\text{GeV}^2$. The D^* meson was required to be in the region $|\eta^{D^*}| < 1.5$ and $p_T^{D^*} > 2\,\text{GeV}$. The D^* meson was included in the jet-finding procedure and was thereby uniquely associated with one jet only. Each jet associated with a D^* was required to satisfy $|\eta^{\rm jet}| < 2.4$ and $E_T^{\rm jet} > 9\,\text{GeV}$.

Cuts on the minimum jet transverse energy and minimum D^* transverse momentum will lead to a bias in the z distribution as $z \sim p^{D^*}/E^{\rm jet}$. Therefore the minimum jet transverse energy was chosen to be as high as possible and the minimum D^* transverse momentum to be as low as possible whilst maintaining statistical precision. With the above requirements, the z distribution is unbiased above 0.22.

5 Fragmentation models

Various parametrisations of fragmentation functions have been proposed. Those considered in this paper are detailed below.

A parametrisation often used to describe the fragmentation of heavy quarks is the function from Peterson et al. [20] which has the form

$$f(z) \propto \frac{1}{[z(1 - 1/z - \epsilon/(1 - z))^2]}\ , \tag{2}$$

where ϵ is a free parameter.

The function from Kartvelishvili et al. [21] has the form

$$f(z) \propto z^{\alpha}(1-z), \tag{3}$$

where α is a free parameter.

Within the framework of the Artru-Mennessier model [22], Bowler [23] developed a fragmentation function for heavy quarks of mass, m_Q, which has the form

$$f(z) \propto \frac{1}{z^{1+r_Q b m_Q^2}} (1-z)^a \exp\left(\frac{-b m_\perp^2}{z}\right), \tag{4}$$

where a and b are free parameters and r_Q is predicted to be unity. The quantity $m_\perp$ is the transverse mass of the hadron, $m_\perp^2 = m^2 + (p_T^{\rm rel})^2$, where m is the hadron's mass and $p_T^{\rm rel}$ the transverse momentum relative to the direction of the quark. The additional freedom given by r_Q allows a smooth transition to the symmetric Lund form [24] ($r_Q \equiv 0$) used to describe light-quark fragmentation.

6 Monte Carlo models

Monte Carlo (MC) models were used both to calculate the acceptance and effects of the detector response and to extract fragmentation parameters. The programmes HERWIG 6.1 [25] and PYTHIA 6.1 [26] which implement LO matrix elements followed by parton showers and hadronisation were used to model the final state. Different parameter settings were used in the MC models when correcting the data or when extracting fragmentation parameters; the settings used when extracting fragmentation parameters are given in Section 8.1. The MC used to correct the data had the default settings, apart from the following changes: the fraction of charged D mesons produced in a vector state was set to 0.6 [27]; and the excited D-meson production rates were set to non-zero values[2] [28].

The ZEUS detector response was simulated in detail using a programme based on GEANT 3.13 [29]. The PYTHIA 6.1 MC programme was used with two different fragmentation schemes: the default which is the Lund string model [30] modified according to Bowler for heavy quarks; and the Peterson fragmentation function with $\epsilon = 0.06$ (see Section 5). The HERWIG 6.1 MC programme uses a cluster model [31] for its fragmentation.

[2] These changes correspond to the PYTHIA parameters: `PARJ(13) = 0.6`, `PARJ(14) = 0.13`, `PARJ(15) = 0.01`, `PARJ(16) = 0.03` and `PARJ(17) = 0.13`.

7 Data correction and systematic uncertainties

The data were corrected for acceptance and effects of detector response using a bin-by-bin method with the PYTHIA simulation used as the central MC. The distribution of the difference in z between hadron and detector levels is symmetric, has a mean of zero and a width of 0.06 units. To maintain both high purity and the validity of the bin-by-bin method, a bin width of at least twice this value (0.14 units) was chosen. The rate due to b quarks was subtracted using the PYTHIA MC prediction normalised to a previous measurement of jet photoproduction [32]. Therefore the cross section as a function of z is for processes in which an initial-state charm quark hadronises to a D^* meson. A detailed analysis [33] of the possible sources of systematic uncertainty was performed. The sources are:

δ_1 the use of an alternative fragmentation model in the PYTHIA MC simulation (see Section 6). As the HERWIG MC simulation gave a poor description of the data, it was not used to correct the data;

δ_2 the b fraction subtracted was changed by (a) +30% and (b) −30% in accordance with the level of agreement between data and PYTHIA MC predictions [32] for jet photoproduction;

δ_3 the total energy in the jet reconstructed from the CAL EFOs was varied by (a) +3% and (b) −3% in the simulation, in accordance with the uncertainty in the jet energy scale;

δ_4 the range of $W_{\gamma p}$ was changed to (a) $124 < W_{\gamma p} < 267\,\text{GeV}$ and (b) $136 < W_{\gamma p} < 293\,\text{GeV}$, in accordance with the resolution;

δ_5 the cut on E_T^{jet} was changed to (a) 10 GeV and (b) 8 GeV, in accordance with the resolution;

δ_6 the value of the cut on $p_T^{D^*}/E_\perp^{\theta>10^\circ}$ was varied to (a) 0.08 and (b) 0.12;

δ_7 the lower (upper) bound on the normalisation region for the wrong-charge candidates was changed to (a) 0.152 ((b) 0.163) GeV.

The cuts on η^{jet}, η^{D^*} and $p_T^{D^*}$ were also varied in accordance with their resolution and produced negligible effects. The values of the above uncertainties for each bin in the normalised cross section, $(1/\sigma)d\sigma/dz$, are given in Table 1. The individual systematic uncertainties were added in quadrature separately for the positive and negative deviations from the nominal cross-section values to obtain the total systematic uncertainties. The systematic uncertainties on the fits of the various fragmentation parametrisations to the data described in Section 8 were obtained from fits to the cross section for each systematic variation. The resulting variations in a given fragmentation parameter were added in quadrature to yield the systematic uncertainty on that parameter.

8 Results

The distributions of the variables z, $p_T^{\rm rel}$, where $p_T^{\rm rel}$ is the transverse momentum of the D^* meson relative to the jet, $p_T^{D^*}$, η^{D^*}, $E_T^{\rm jet}$ and $\eta^{\rm jet}$ are shown in Fig. 2 and compared to the distributions from the MC programmes, normalised to the data. Also shown is the prediction of the PYTHIA simulation for the production of beauty quarks subsequently producing a D^* meson; this amounts to about 6%. The z distribution is reasonably well described by the PYTHIA MC predictions, whereas the HERWIG prediction does not describe the data. This can be seen in the differences between the measured $p_T^{D^*}$ distribution and that predicted by HERWIG. The MC predictions for the $E_T^{\rm jet}$ distribution are, however, similar and agree reasonably well with the measurement. For the $p_T^{\rm rel}$ distribution, the PYTHIA simulations give a good description of the data and are again better than that from HERWIG. This shows that the PYTHIA MC model using both the Bowler and Peterson fragmentation for charm quarks gives a good description of the transverse as well as the longitudinal component of the D^* fragmentation process. The distribution of the pseudorapidities of both jet and D^* are similarly well described by both MC programmes. As the HERWIG MC model is known to give a better description than PYTHIA of data [34] sensitive to the parton-shower model, the differences shown here suggest that the cluster model does not describe the hadronisation process of charm quarks to D^* mesons.

The normalised differential cross section, $1/\sigma(d\sigma/dz)$, is presented in the kinematic region $Q^2 < 1\,\text{GeV}^2$ and $130 < W_{\gamma p} < 280\,\text{GeV}$, requiring at least one jet with $E_T^{\rm jet} > 9\,\text{GeV}$ and $|\eta^{\rm jet}| < 2.4$. A D^* meson with $p_T^{D^*} > 2\,\text{GeV}$ and $|\eta^{D^*}| < 1.5$ was required to be associated with any jet that satisfied the above jet requirements on $E_T^{\rm jet}$ and $\eta^{\rm jet}$. The D^* meson was included in the jet-finding procedure and was thereby uniquely associated with one jet only. The values of the cross section are given in Table 2 and shown in Figs. 3 and 4 compared to various expectations. In Fig. 5, the same data are shown compared with results from e^+e^- experiments.

8.1 Comparison with fragmentation models in PYTHIA

The normalised cross section is shown in Fig. 3 compared to the PYTHIA MC simulation using different fragmentation models. The original default settings for PYTHIA 6.1 were used with the proton and photon parton density functions set to GRV94 LO [35] and GRV-LO [36], respectively and a different value for the maximum parton virtuality allowed in space-like showers (`PARP(67)` in PYTHIA changed from 1.0 to 4.0 [37]). Otherwise, only the fragmentation parameters considered (see Section 5) were varied.

The default fragmentation setting in the simulation is the symmetric Lund string fragmentation modified for heavy quarks according to Bowler (see Eq. 4). Three predictions

for different values of r_Q are shown compared to the data in Fig. 3(a). The default prediction with $r_Q = 1$ gives a reasonable description of the data; as r_Q decreases, the prediction deviates more and more from the data.

The Peterson function (see Eq. 2) and the option to vary ϵ is available within the PYTHIA simulation. The value of ϵ was varied in the range 0.01 to 0.1, with the Lund string fragmentation model used for lighter flavours. For each value in the MC simulation, the full event record was generated and the kinematic requirements applied, allowing a direct comparison to the data. The result of varying ϵ is shown in Fig. 3(b). Here it can be seen that values as low as $\epsilon = 0.01$ are disfavoured, producing a much harder spectrum than the data, while values as high as $\epsilon = 0.1$ result in too soft a spectrum and are therefore also disfavoured. The result of fitting the MC to the data was $\epsilon = 0.062 \pm 0.007^{+0.008}_{-0.004}$ where the first uncertainty is statistical and the second systematic. The value is consistent with the default value in the MC of $\epsilon = 0.05$ which was obtained from comparisons [26] with LEP and SLD data at the Z^0 mass. The fitted value was then used in the MC and the result compared in Fig. 3(b); the data are well described.

8.2 Comparison with next-to-leading-order QCD calculations

The data were compared with a next-to-leading-order (NLO) QCD prediction [38] which is a fixed-order calculation from Frixione et al. (FMNR). As default, the programme is interfaced to the Peterson fragmentation function; the function from Kartvelishvili et al. (see Eq. 3) was also implemented. The other parameters used in the NLO QCD calculation were as follows: the renormalisation and factorisation scales were set to $\mu = \sqrt{\langle (p_T^c)^2 \rangle + m_c^2}$, where $\langle (p_T^c)^2 \rangle$ is the average squared transverse momentum of the two charm quarks and $m_c = 1.5\,\text{GeV}$; the proton parton density function was CTEQ5M1 [39]; and the photon parton density function was AFG-HO [40].

As the final state particles in the NLO QCD calculation are partons, to enable a fair comparison with the data, the predictions were corrected for effects of hadronisation using a bin-by-bin procedure according to $\Delta\sigma = \Delta\sigma^{\text{NLO}} \cdot C_{\text{had}}$, where $\Delta\sigma^{\text{NLO}}$ is the cross section for partons in the final state of the NLO calculation. The hadronisation correction factor, C_{had}, was defined as the ratio of the cross sections after and before the hadronisation process, $C_{\text{had}} = \Delta\sigma_{\text{MC}}^{\text{Hadrons}} / \Delta\sigma_{\text{MC}}^{\text{Partons}}$, where the partons used are those after parton showering. The values of C_{had} from PYTHIA were used for the central results. As the results of HERWIG do not describe the data (see Section 6), they are used only as a systematic check. The prediction from this combination of NLO QCD and hadronisation correction is termed "FMNR$\times C_{\text{had}}^{\text{PYT}}$". The values of C_{had} are given for PYTHIA and HERWIG in Table 2.

The result of varying ϵ in the Peterson function and α in the Kartvelishvili function for the predictions of FMNR$\times C_{\rm had}^{\rm PYT}$ are shown in Figs. 4(a) and (b), respectively. The data again show sensitivity to these fragmentation functions and can constrain their free parameters. The results of fits to the data are $\epsilon = 0.079 \pm 0.008^{+0.010}_{-0.005}$ and $\alpha = 2.67 \pm 0.18^{+0.17}_{-0.25}$ for the Peterson and Kartvelishvili functions, respectively, where the first uncertainty is statistical and the second systematic.

A number of parameter settings which are commonly used in comparison with data [34] were considered. Using $C_{\rm had}$ from HERWIG gave $\epsilon = 0.094 \pm 0.008$ and $\alpha = 2.46 \pm 0.17$, where the uncertainty is statistical only. The effect of the input parameters in the NLO QCD programme was checked by changing the renormalisation scale and charm mass simultaneously to 2μ and 1.7 GeV and 0.5μ and 1.3 GeV. The different settings gave values of ϵ (α) of 0.082 (2.55) and 0.077 (2.80), respectively; the uncertainty from the NLO QCD input parameters is significantly smaller than the experimental uncertainties.

The default ϵ value used so far in NLO QCD calculations, extracted from a fit [41] to ARGUS [42] data, was 0.035. As the perturbative part of the production in calculations of e^+e^- and ep cross sections depends on the scale of the process and colour connections between the outgoing quarks and the proton remnant can have an effect, the values of ϵ extracted with NLO QCD from e^+e^- and ep data may not necessarily be the same. This illustrates that care is needed in choosing the appropriate fragmentation parameter.

8.3 Measurement of $\langle z \rangle$ and comparisons with e^+e^- data

In Fig. 5, the ZEUS data are shown compared with measurements from the Belle [3], CLEO [2] and ALEPH [4] collaborations in e^+e^- interactions. The Belle and CLEO data are measured at a similar centre-of-mass energy of about 10.5 GeV, whereas the ALEPH data was taken at 91.2 GeV. The corresponding scale of the ZEUS data is given by twice the average transverse energy of the jet, 23.6 GeV, and is between the two e^+e^- centre-of-mass energies.

Although using a different definition for z, the general features of the data presented here are similar to those at e^+e^- experiments. However the ZEUS data are shifted somewhat to lower values of z compared to the CLEO and Belle data with the ALEPH data even lower. This can be seen more quantitatively by extracting the mean value of the distribution, $\langle z \rangle = 0.588 \pm 0.025\,(\text{stat.}) \pm 0.029\,(\text{syst.})$. The PYTHIA MC programme was used to extrapolate the phase space to $p_T^{D^*} = 0$ and to correct for the subsequent exclusion of the region $0 < z < 0.16$. It was also used to correct for the finite bin size. The resulting factor was 0.961. The corrected value,

$$\langle z \rangle = 0.565 \pm 0.024\,(\text{stat.}) \pm 0.028\,(\text{syst.}) \tag{5}$$

and those from ALEPH, Belle and CLEO are shown in Table 3. It should be noted that the ALEPH data uses the beam energy as the scale rather than the jet energy which, due to hard gluon emission, would be a better equivalent to the jet energy used in this analysis. The usage of jet energy for ALEPH data would lead to an increase in $\langle z \rangle$. Although the uncertainties on the current measurement are larger than those from the e^+e^- experiments, the value is qualitatively consistent with expectations from scaling violations in QCD in which $\langle z \rangle$ decreases with increasing energy [43].

9 Summary

The fragmentation function for D^* mesons has been measured in photoproduction at HERA using the variable $z = (E + p_{\|})^{D^*}/2E^{\text{jet}}$ and requiring a jet with $E_T^{\text{jet}} > 9\,\text{GeV}$ and $|\eta^{\text{jet}}| < 2.4$ to be associated with a D^* meson in the range $p_T^{D^*} > 2\,\text{GeV}$ and $|\eta^{D^*}| < 1.5$.

The data are compared to different fragmentation models in MC simulations and a NLO QCD calculation. The cluster model used in the HERWIG programme does not describe the data. Within the framework of NLO QCD and the PYTHIA simulation, the free parameters of the Peterson fragmentation function and, for NLO QCD, the Kartvelishvili function have been fitted.

The value of ϵ in the Peterson function, extracted within the framework of NLO QCD, is different to that extracted using data from e^+e^- collisions. As the perturbative aspects of the corresponding calculations and the energy scales are different, the results are not expected to be the same. Future calculations of charm hadron cross sections at NLO QCD at HERA should always use the appropriate values. Within the consistent framework given by the PYTHIA model, the extracted fragmentation parameters agree with those determined in e^+e^- data.

The fragmentation function and the $\langle z \rangle$ are different to those measured at different centre-of-mass energies in e^+e^- collisions; the measured $\langle z \rangle$ is higher than the ALEPH data and lower than the CLEO and Belle data, qualitatively consistent with the scaling of this variable as predicted by QCD.

Acknowledgements

We thank the DESY Directorate for their strong support and encouragement. The remarkable achievements of the HERA machine group were essential for the completion of

this work and are greatly appreciated. The design, construction and installation of the ZEUS detector was made possible by the efforts of many people who are not listed as authors.

References

[1] J. Braciník et al., *HERA and the LHC: A workshop on the implications of HERA for LHC physics*, A. De Roeck and H. Jung (eds.), Vol. B, p. 390. Geneva, CERN/DESY (2005), and references therein.

[2] CLEO Coll., M. Artuso et al., Phys. Rev. **D 70**, 112001 (2004).

[3] Belle Coll., R. Seuster et al., Phys. Rev. **D 73**, 032002 (2006).

[4] ALEPH Coll., R. Barate et al., Eur. Phys. J. **C 16**, 597 (2000).

[5] B. Mele and P. Nason, Nucl. Phys. **B 361**, 626 (1991).

[6] V.N. Gribov and L.N. Lipatov, Sov. J. Nucl. Phys. **15**, 438 (1972);
L.N. Lipatov, Sov. J. Nucl. Phys. **20**, 94 (1975);
G. Altarelli and G. Parisi, Nucl. Phys. **B 126**, 298 (1977);
Yu.L. Dokshitzer, Sov. Phys. JETP **46**, 641 (1977).

[7] H1 Coll., F.D. Aaron et al., Eur. Phys. J. **C 59**, 589 (2009).

[8] ZEUS Coll., U. Holm (ed.), *The ZEUS Detector*. Status Report (unpublished), DESY (1993), available on `http://www-zeus.desy.de/bluebook/bluebook.html`.

[9] N. Harnew et al., Nucl. Inst. Meth. **A 279**, 290 (1989);
B. Foster et al., Nucl. Phys. Proc. Suppl. **B 32**, 181 (1993);
B. Foster et al., Nucl. Inst. Meth. **A 338**, 254 (1994).

[10] M. Derrick et al., Nucl. Inst. Meth. **A 309**, 77 (1991);
A. Andresen et al., Nucl. Inst. Meth. **A 309**, 101 (1991);
A. Caldwell et al., Nucl. Inst. Meth. **A 321**, 356 (1992);
A. Bernstein et al., Nucl. Inst. Meth. **A 336**, 23 (1993).

[11] J. Andruszków et al., Preprint DESY-92-066, DESY, 1992;
ZEUS Coll., M. Derrick et al., Z. Phys. **C 63**, 391 (1994);
J. Andruszków et al., Acta Phys. Pol. **B 32**, 2025 (2001).

[12] W.H. Smith, K. Tokushuku and L.W. Wiggers, *Proc. Computing in High-Energy Physics (CHEP), Annecy, France, Sept. 1992*, C. Verkerk and W. Wojcik (eds.), p. 222. CERN, Geneva, Switzerland (1992). Also in preprint DESY 92-150B.

[13] ZEUS Coll., J. Breitweg et al., Eur. Phys. J. **C 1**, 109 (1998).

[14] ZEUS Coll., J. Breitweg et al., Eur. Phys. J. **C 6**, 43 (1999);
G.M. Briskin, Ph.D. Thesis, Tel Aviv University, Report DESY-THESIS-1998-036, 1998.

[15] S. Catani et al., Nucl. Phys. **B 406**, 187 (1993).

[16] S.D. Ellis and D.E. Soper, Phys. Rev. **D 48**, 3160 (1993).

[17] ZEUS Coll., M. Derrick et al., Phys. Lett. **B 322**, 287 (1994).

[18] S. Nussinov, Phys. Rev. Lett. **35**, 1672 (1975);
G.J. Feldman et al., Phys. Rev. Lett. **38**, 1313 (1977).

[19] ZEUS Coll., J. Breitweg et al., Eur. Phys. J. **C 6**, 67 (1999).

[20] C. Peterson et al., Phys. Rev. **D 27**, 105 (1983).

[21] V.G. Kartvelishvili, A.K. Likhoded and V.A. Petrov, Phys. Lett. **B 78**, 615 (1978).

[22] X. Artru and G. Mennessier, Nucl. Phys. **B 70**, 93 (1974).

[23] M.G. Bowler, Z. Phys. **C 11**, 169 (1981).

[24] B. Andersson, G. Gustafson and B. Söderberg, Z. Phys. **C 20**, 317 (1983).

[25] G. Marchesini et al., Comp. Phys. Comm. **67**, 465 (1992).

[26] T. Sjöstrand, Comp. Phys. Comm. **135**, 238 (2001).

[27] ZEUS Coll., S. Chekanov et al., Eur. Phys. J. **C 44**, 351 (2005).

[28] ZEUS Coll., S. Chekanov et al., Eur. Phys. J. **C 60**, 25 (2009).

[29] R. Brun et al., GEANT3, Technical Report CERN-DD/EE/84-1, CERN (1987).

[30] B. Andersson et al., Phys. Rep. **97**, 31 (1983).

[31] B.R. Webber, Nucl. Phys. **B 238**, 492 (1984).

[32] ZEUS Coll., S. Chekanov et al., Phys. Rev. **D 70**, 012008 (2004).

[33] S. Padhi, Ph.D. Thesis, McGill University, Montreal, Report DESY-THESIS 2004-012, 2004.

[34] ZEUS Coll., S. Chekanov et al., Nucl. Phys. **B 729**, 492 (2005).

[35] M. Glück, E. Reya and A. Vogt, Z. Phys. **C 67**, 433 (1995).

[36] M. Glück, E. Reya and A. Vogt, Phys. Rev. **D 46**, 1973 (1992).

[37] J.M. Butterworth and M. Wing, Rep. Prog. Phys. **68**, 2773 (2005).

[38] S. Frixione et al., Phys. Lett. **B 348**, 633 (1995);
S. Frixione, P. Nason and G. Ridolfi, Nucl. Phys. **B 454**, 3 (1995).

[39] CTEQ Coll., H.L. Lai et al., Eur. Phys. J. **C 12**, 375 (2000).

[40] P. Aurenche, J.P. Guillet and M. Fontannaz, Z. Phys. **C 64**, 621 (1994).

[41] P. Nason and C. Oleari, Nucl. Phys. **B 565**, 245 (2000).

[42] ARGUS Coll., H. Albrecht et al., Z. Phys. **C 52**, 353 (1991).

[43] M. Cacciari, P. Nason and C. Oleari, JHEP **0604**, 006 (2006).

Source	z bin (0.16, 0.30)	(0.30, 0.44)	(0.44, 0.58)	(0.58, 0.72)	(0.72, 0.86)	(0.86, 1)
δ_1 (%)	+17.0	−1.9	−6.4	+3.2	+8.8	−21.0
δ_{2a} (%)	+8.4	+2.2	−1.0	−1.0	−1.8	−2.2
δ_{2b} (%)	+7.0	−2.2	+0.9	+0.9	+1.7	+2.0
δ_{3a} (%)	+1.4	−5.8	+0.3	+1.2	+1.6	+3.1
δ_{3b} (%)	+4.1	+2.9	+0.4	−0.1	−3.4	−2.7
δ_{4a} (%)	−2.9	+5.3	−0.3	+3.0	−2.0	−11.0
δ_{4b} (%)	+14.0	−1.8	−1.1	−0.5	−0.8	−2.6
δ_{5a} (%)	−6.8	+3.6	−1.9	+2.5	+5.9	−16.0
δ_{5b} (%)	−29.0	−7.9	+2.1	+12.0	−0.6	+4.9
δ_{6a} (%)	−39.0	+6.1	+2.7	+2.3	+2.3	+2.3
δ_{6b} (%)	+37.0	−3.3	−3.5	−2.7	−2.4	−2.4
δ_{7a} (%)	−0.3	+0.3	+0.5	−0.5	−0.3	−0.8
δ_{7b} (%)	−1.7	+1.1	−0.1	−0.3	+0.4	−1.7

Table 1: *Individual sources of systematic uncertainty (in %) per bin of the normalised cross-section $(1/\sigma)d\sigma/dz$. The description of each variation is given in Section 7.*

z bin	$(1/\sigma)d\sigma/dz$	$\delta_{\rm stat}$	$\delta_{\rm syst}$	$C_{\rm had}^{\rm PYT}$	$C_{\rm had}^{\rm HRW}$
0.16, 0.30	0.53	$\pm$ 0.19	$^{+0.23}_{-0.26}$	1.82	1.43
0.30, 0.44	1.26	$\pm$ 0.17	$^{+0.12}_{-0.14}$	1.58	1.08
0.44, 0.58	1.67	$\pm$ 0.15	$^{+0.06}_{-0.13}$	1.28	1.00
0.58, 0.72	1.68	$\pm$ 0.14	$^{+0.22}_{-0.05}$	1.18	0.91
0.72, 0.86	1.36	$\pm$ 0.12	$^{+0.15}_{-0.07}$	1.02	0.85
0.86, 1	0.63	$\pm$ 0.08	$^{+0.04}_{-0.18}$	1.33	1.16

Table 2: *Measured normalised cross-section $(1/\sigma)d\sigma/dz$. The statistical ($\delta_{\rm stat}$) and systematic ($\delta_{\rm syst}$) uncertainties are shown separately. The bin-by-bin corrections for hadronisation (see Section 8.2) are shown for* Pythia, $C_{\rm had}^{\rm PYT}$, *and* Herwig, $C_{\rm had}^{\rm HRW}$.

Collaboration	Scale (GeV)	Measured variable	$\langle z \rangle \pm$ stat. $\pm$ syst.
ALEPH	91.2	$\langle E^{D^*}/E^{\mathrm{beam}} \rangle$	$0.4878 \pm 0.0046 \pm 0.0061$
Belle	10.6	$\langle p^{D^*}/p^{\mathrm{max}} \rangle$	$0.61217 \pm 0.00036 \pm 0.00143$
CLEO	10.5	$\langle p^{D^*}/p^{\mathrm{max}} \rangle$	$0.611 \pm 0.007 \pm 0.004$
ZEUS	23.6	$\langle (E + p_{\parallel})^{D^*}/2E^{\mathrm{jet}} \rangle$	$0.565 \pm 0.024 \pm 0.028$

Table 3: *Mean value, $\langle z \rangle$, of the fragmentation function in e^+e^- collisions, ALEPH, Belle and CLEO, compared with the measurement in this paper. The statistical and systematic uncertainties are shown separately.*

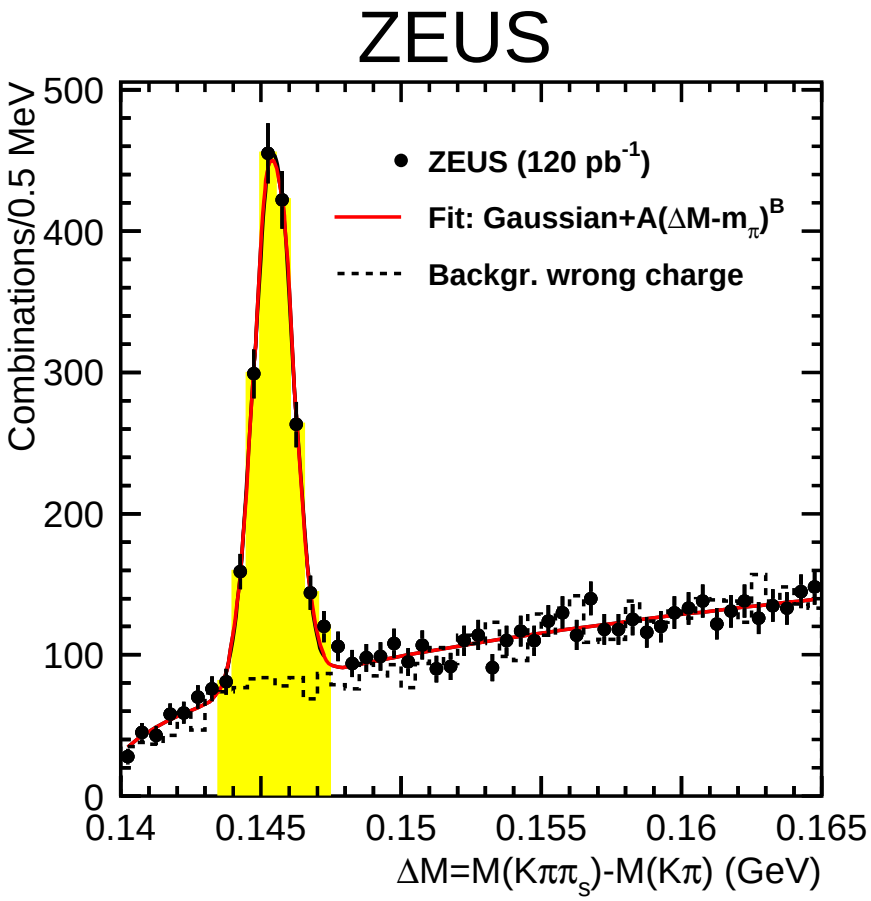

Figure 1: *The distribution of the mass difference, ΔM, showing the right-charge combinations (points) and wrong-charge combinations (dashed histogram). The shaded area shows the signal region, $0.1435 < \Delta M < 0.1475\,GeV$. The solid line is a fit to a Gaussian function plus $A(\Delta M - m_\pi)^B$ to describe the background, where A and B are constants.*

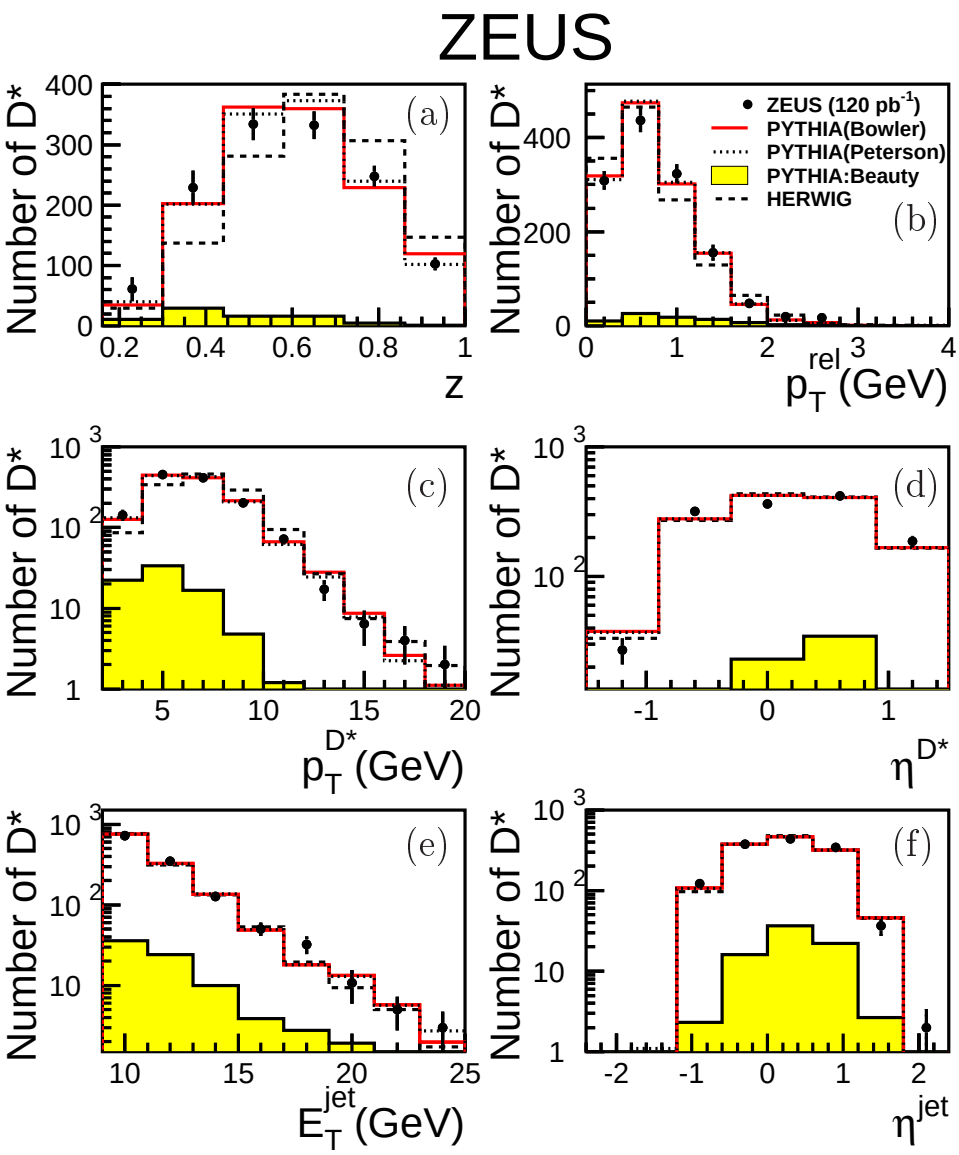

Figure 2: *Distributions of number of D^* mesons versus (a) z, (b) $p_T^{\rm rel}$, (c) $p_T^{D^*}$, (d) η^{D^*}, (e) $E_T^{\rm jet}$ and (f) $\eta^{\rm jet}$ for data (points) and MC simulations. The data are compared with* PYTHIA *using the Bowler (solid line) and Peterson, with $\epsilon = 0.06$, (dotted line) fragmentation functions and with* HERWIG *(dashed line). The component of beauty production as predicted by* PYTHIA *(shaded histogram) is also shown.*

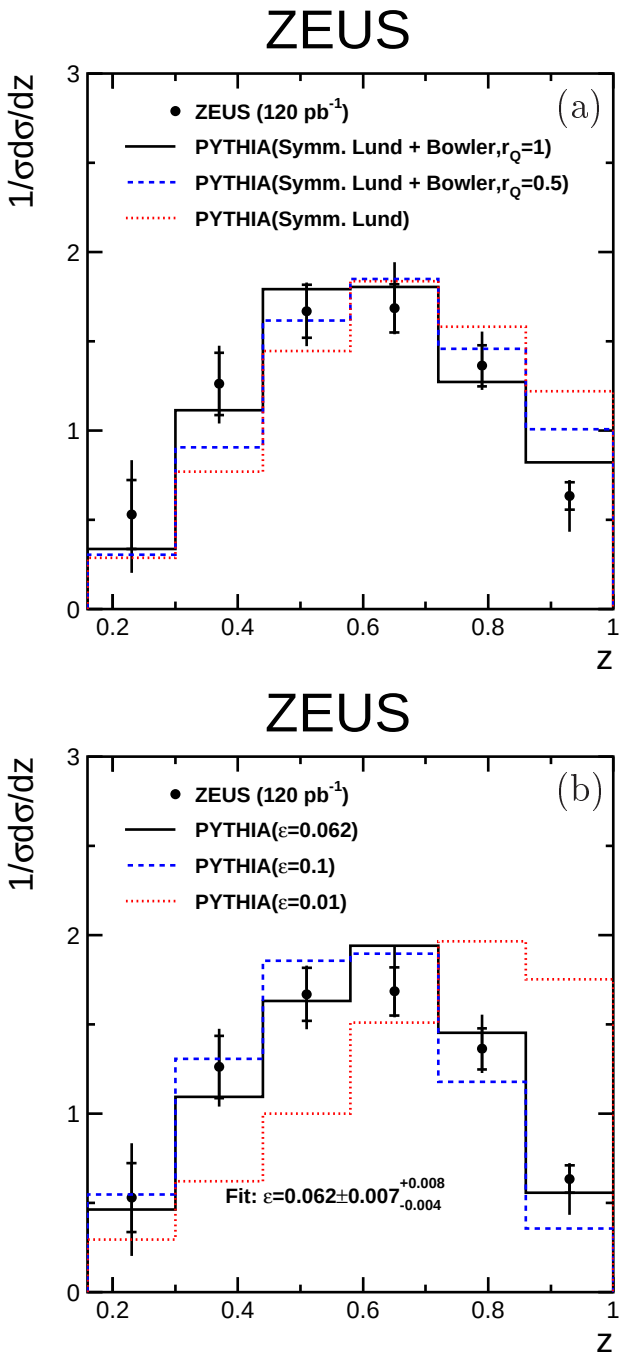

Figure 3: *Normalised cross section, $1/\sigma(d\sigma/dz)$, for the data (points) compared with (a) the symmetric Lund fragmentation modified for heavy quarks (see Eq. 4) with $r_Q = 1$ (solid line), $r_Q = 0.5$ (dashed line) and the original symmetric Lund scheme, $r_Q = 0$, (dotted line) as implemented in* PYTHIA. *The data are also compared with (b) the Peterson fragmentation function with values of the parameter $\epsilon = 0.1$ (dashed line), $\epsilon = 0.01$ (dotted line) and the fitted value $\epsilon = 0.062$ (solid line) as implemented in* PYTHIA.

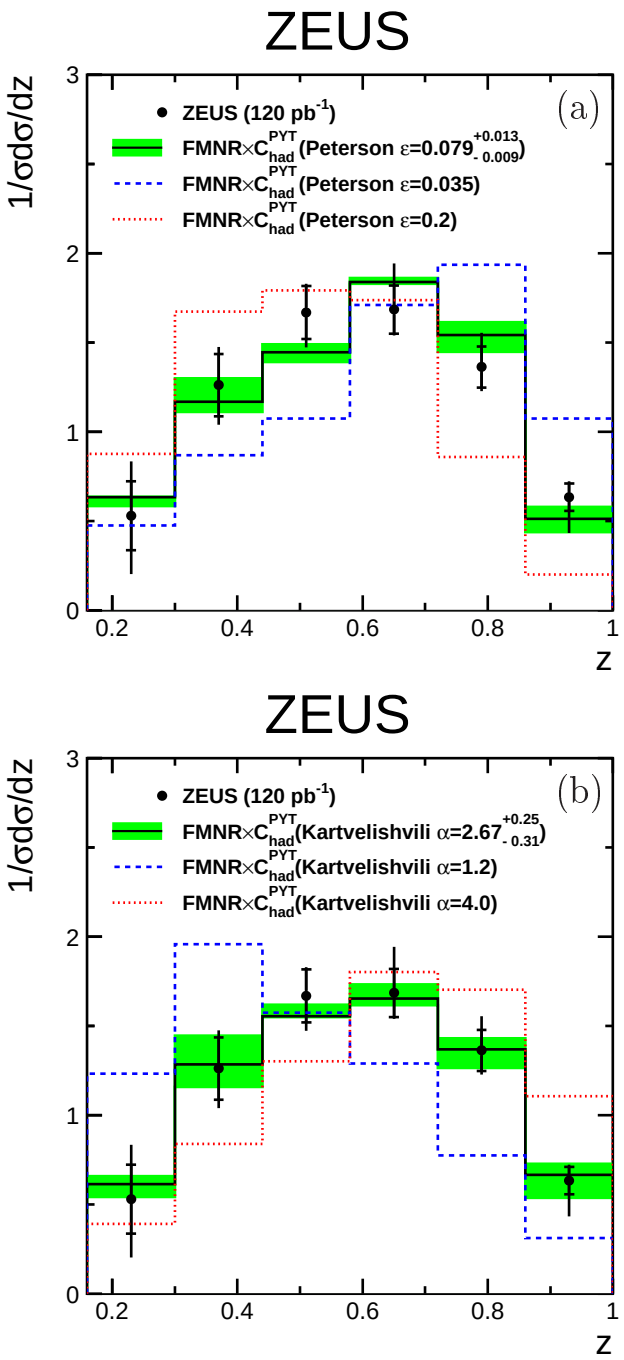

Figure 4: *Normalised cross section, $1/\sigma(d\sigma/dz)$, for the data (points) compared with the predictions of $FMNR{\times}C_{\rm had}^{\rm PYT}$. (a) the Peterson fragmentation function in the calculation is shown with $\epsilon = 0.2$ (dotted line), $\epsilon = 0.035$ (dashed line) and the fitted value $\epsilon = 0.079^{+0.013}_{-0.009}$ (stat.$\oplus$syst.) (solid line). (b) the Kartvelishvili fragmentation function in the calculation is shown with $\alpha = 1.2$ (dashed line), $\alpha = 4.0$ (dotted line) and the fitted value $\alpha = 2.67^{+0.25}_{-0.31}$ (stat.$\oplus$syst.) (solid line). The fitted $FMNR{\times}C_{\rm had}^{\rm PYT}$ predictions are shown with the experimental uncertainties of the fit (shaded band).*

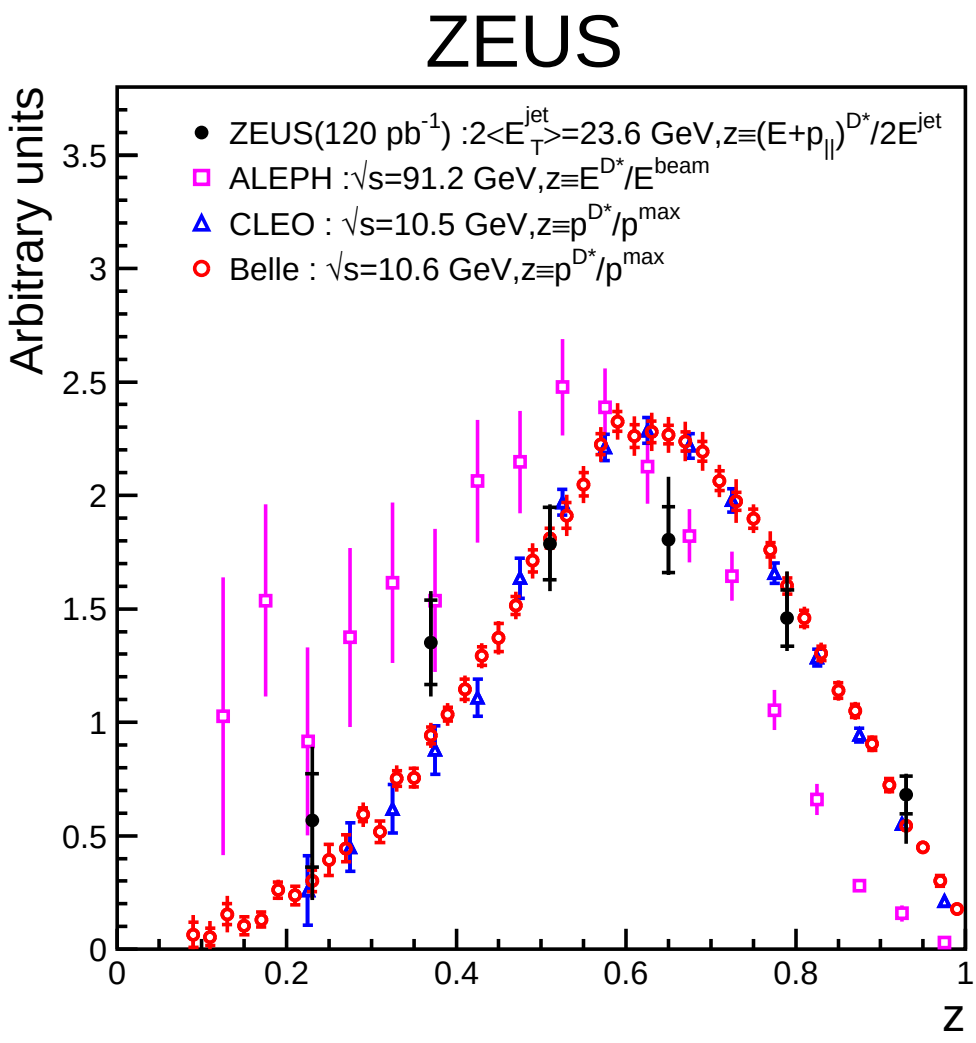

Figure 5: *D^* fragmentation function for the ZEUS data (solid points) compared to measurements of the Belle (open circles), CLEO (open triangles) and ALEPH (open squares) collaborations in e^+e^- collisions. For shape comparison, the data sets were normalised to 1/(bin width) for $z > 0.3$. For the ALEPH data, the fragmentation function is measured versus the ratio of the energy of the D^* meson and the beam energy, whereas for the Belle and CLEO data, the fragmentation function is measured versus the ratio of the momentum of the D^* meson and the maximum attainable momentum at the relevant beam energy.*